Real-Time Infrared Determination of Photoinitiated Copolymerization Reactivity Ratios: Application of the Hilbert Transform and Critical Evaluation of Data Analysis Techniques

Johan F. G. A. Jansen,* Erwin E. J. E. Houben, Peter H. G. Tummers, Dietrich Wienke, and John Hoffmann

DSM Research, P.O. Box 18, 6160 MD Geleen, The Netherlands

Received October 21, 2003; Revised Manuscript Received January 19, 2004

ABSTRACT: The reactivity ratios of various UV-copolymerizing systems were determined employing RT-FTIR spectroscopy, combined with advanced and alternative multivariate-statistical data analysis techniques. For complex mixtures peak identification as well as peak deconvolution has been increased significantly by employment of 2-dimensional correlation spectroscopy, based on the Hilbert transform. As an advantage, kinetic reaction profiles of homo- and copolymerization reactions have been extracted and have been separated without any additional measurement. The following reactivity ratios were obtained: fumarate/vinyl ether $r_1 = 0$, $r_2 = 0$; maleate/vinyl ether $r_1 = 0$, $r_2 = 0$; fumarate/allyl ether $r_1 = 0$, $r_2 = 0$; maleate/allyl ether $r_1 = 0$, $r_2 = 0$; fumarate/methacrylate $r_1 = 0$, $r_2 = 1.3$; fumarate/acrylate $r_1 = 0$, $r_2 > 50$; methacrylate/vinyl ether $r_1 = 16$, $r_2 = 0$; methacrylate/allyl ether $r_1 > 100$, $r_2 = 0$; methacrylate/acrylate $r_1 = 1.6$, $r_2 = 0.15$; methacrylate/*N*-vinylcaprolactam $r_1 = 7.3$, $r_2 = 0.01$; and acrylate/*N*-vinylcaprolactam $r_1 = 1.3$, $r_2 = 0.01$. Kinetically, the fumarate−vinyl ether copolymerization can be regarded as the homopolymerization of a CT complex while the fumarate allyl ether copolymerization should be regarded as a perfect alternating copolymerization. The HEA−NVC copolymerization has to be regarded as a terpolymerization between HEA, NVC, and the HEA−NVC charge-transfer complex.

Introduction

The photoinitiated polymerization of methacrylates and acrylates is one of the most efficient and facile processes for the rapid production of polymeric cross-linked materials, especially materials with well-defined properties. Therefore, this technique is widely employed in the coating industries in which a high demand is put on the mechanical properties as well as on the optical properties of the materials. Well-known examples are for instance dental restorative fillers, fiber-optic coatings, aspherical lenses for CD applications, the preparation of contact lenses, and stereolithography for rapid prototyping.[1] The kinetics of these homopolymerizations has been studied in detail[2] using photoinitiated differential scanning calorimetry (photo-DSC) and real-time Fourier transform infrared spectroscopy (RT-FTIR). These investigations have led to several kinetic models like bimolecular termination combined with reaction diffusion-controlled kinetics,[3] monomolecular termination in the glassy region,[4] primary radical termination,[5] chain length dependent termination,[6] random walk for heterogeneity,[7] primary cyclization,[8] and the effect of monomer functionality.[9]

In principle, mid-infrared spectroscopy,[10] especially real-time infrared (RT-IR), is very suitable for studying copolymerizations as well. An eminent advantage of the use of RT-FTIR spectroscopy is that a single experiment could in principle be sufficient for the determination of the reactivity ratios. In theory, the only constraint is that the theoretical feed composition should change upon polymerization. So only in the case of azeotropic copolymerizations multiple feed compositions have to be prepared for the correct determination of the reactivity ratios. To the best of our knowledge, the only examples described in the literature of photoinitiated copolymerizations are performed on formulations of which the IR signals are baseline resolved as such. For these copolymerizations,[11] different maleate−vinyl ether mixtures and different fumarate−vinyl ether mixtures all the determined reactivity ratios were 0. Exploiting the advantage of using a real-time analysis, i.e., being able to obtain the full kinetic data simultaneously, Decker was able to demonstrate that these copolymerizations were in fact homopolymerizations of a maleate−vinyl ether or fumarate−vinyl ether charge-transfer complex.[11a] Later maleimide−vinyl ether copolymerizations were studied as well.

However, one should be aware of the fact that the dynamic formation of the photoresin under UV radiation leads to a continuous change in the chemical environment of the remaining uncured monomer. Examples for such a dynamic changing chemical environment are sample thickness shrinkage, sample density change, and network formation. This again leads to a dynamic change in chemical activity for the monomer having finally an impact on the quality of the dynamic real-time FT-IR spectra. Sample shrinkage reduces optical path length, and therefore reduced absorption as well changes in baseline position can occur. However, this might be compensated by the increased concentration upon shrinkage. Change in resin density and composition has impact on refractive index, which can change peak shape and baseline position, too. Change in chemical activity can cause peak position shifts along the wavenumber axis. Change in chemical activity can also cause a change in absorption coefficient. On top of that, and depending on the photochemical mixture under study, sometimes spectral interferences can occur, causing undesired spectral peak overlap. As a result of this spectral overlap, RT-FTIR has been seldom used for the

* To whom correspondence should be addressed: e-mail johan-fga.jansen@dsm.com.

10.1021/ma035587r CCC: $27.50
Published on Web 02/25/2004

determination of reactivity ratios due to the fact that overlapping IR signals could make it difficult to accurately determine the composition of a formulation at a given time.[12] Furthermore, in many of the interesting mixtures for which real-time infrared analysis could be used in order to determine the reactivity ratios, the infrared absorptions of the double bonds involved are indeed not well resolved or simply interfering. Facing interfering double-bond signals in the IR spectra the first option is to identify absorptions, which although not originating from the polymerizing bonds can be attributed unambiguously to one of the components and are still well resolved. As an alternative, the overlapping double bond absorptions can be resolved by using deconvolution techniques like first- or second-derivative peak model fitting. However, if the signals are close together, it will be very difficult to establish which component reacts first. Fortunately, a spectral data set recorded during such a single RT-FTIR experiment is inherently multivariate structured. Thus, new multivariate analytical algorithms, e.g., 2D correlation spectroscopy, could boost the usability dramatically. Employment of 2D correlation spectroscopy provides a good indication which component reacts predominantly first as well as the exact peak positions in a reacting mixture (in principle required for a correct deconvolution procedure). Other analytical data evaluation techniques are for instance the univariate method,[13] peak fitted deconvolution,[14] and multivariant techniques like SIMPLISMA[15] (simple to use interactive self-modeling mixture analysis) and multivariate curve resolution (MCR).[16,17] An often unmentioned requirement is that all the different analytical techniques should yield the same result, as the reactivity ratios do not depend on the method of data treatment. Taking into account the sampling and specific sample problems, listed above, it has been considered worthwhile to start a critical evaluation of different advanced multivariate data analysis techniques for determination of the reactivity ratios of various photoinitiated copolymerizations. The present paper then aims to advise a data analysis strategy for dynamic real-time spectra, which are obtained from UV-photo-copolymerization experiments.

Experimental Section

Materials. All the monomers studied, i.e., dibutyl fumarate, dibutyl maleate, hydroxyethyl vinyl ether, hydroxyethyl allyl ether, hydroxyethyl acrylate (HEA), hydroxyethyl methacrylate (HEMA), ethyl-α-hydroxy methacrylate (EHMA), and *N*-vinylcaprolactam (NVC), were obtained from Aldrich or other sources and freshly distilled before use. The prime purpose of this distillation is inhibitor removal. The hydroxy esters, e.g. HEA, HEMA, and EHMA, can contain divinyl compounds (formed via transesterfication reactions), which can have a large impact on the cure kinetics since a cross-linked network could be formed. To circumvent these possible problems, these monomers were, after the inhibitor removing distillation, distilled twice using large spills and a cooled collecting bulb (−18 °C), after which the samples are stored cold (4 °C). In this way the setting of the transesterfication equilibrium is postponed. Up to 1 week after distillation, based on GC, still no divinyls could be observed while without the two additional distillations sometimes up to 0.5% divinyl could be detected (assuming the same response factors). Although these minor impurities could have a large impact on the overall kinetics (earlier onset of reaction diffusion-controlled kinetics), we did not detect an influence of these traces of divinyls on the reactivity ratios.

The RT-FTIR setup employed is described in detail elsewhere.[19] A 200 W D-bulb (Dr. Honle) was used as source or irradiation, resulting in an intensity of approximately 40 mW/cm^2 at the sample position (average of three measurements), as measured with a Solatell Sola-scope 1. It should be noted that in contrast to most published RT-FTIR measurements the samples were not measured as laminates but under an inert atmosphere in a transmission reflection setup employing approximately 7 μm thick samples. Nitrogen was purged for at least 5 min before any RT-IR measurement. All RT-IR measurements were performed in triplicate, with a maximum spectral sampling rate of 0.038 s per IR spectrum (at 4 cm^{-1} spectral resolution). In case slower polymerizations were monitored higher spectral resolutions up to 0.2 cm^{-1} were used. All RT-IR measurements were performed employing 1 wt % Irgacure 184 (2-hydroxycyclohexyl phenyl ketone, HCPK, Ciba) as the photoinitiator. All photoinitiated polymerizations were performed to an extent of >96%, curing of one of the components (based on IR). Table 1 shows the IR frequencies that were employed for the determination of the conversion levels.

Table 1. Characteristic Frequencies of Reactive Groups

	freq for vibrational modes (cm^{-1})		
functional group	C−H def	C=C str	C−H str
acrylate	810, 985, 1410	1635	3104
methacrylate	815, 939	1640	3080
alkoxy methacrylate	820	1638	3080
vinyl ether	840	1618	3120
allyl ether	910, 990	1645	3080
fumarate	775, 979	1646	
maleate	850, 1406	1645	
N-vinyl		1670	

^{1}H and ^{13}C NMR spectra were recorded on a Bruker AMX-200 using $CDCl_3$ as solvent

Description of Univariate Method. This data analysis technique is the most straightforward method used for extracting kinetic data out of real-time FTIR experiments. The method was first described by Decker[13] where the peak height of a functional group specific vibrational band is monitored. This method has been extended by applying a baseline correction before determination of the peak height. The conversion level, *C*, at every time point can be calculated using the formula

$$C\,(\%) = \frac{A_0 - A_x}{A_0} \times 100\%$$

where A_0 and A_x are the net absorbencies in the first FTIR spectrum and the FTIR spectrum at time point *x*, respectively. The conversion plotted against the reaction time shows a profile that visualizes how specific functional groups are consumed and built into a polymer. For each type of functional group a reaction profile can be obtained out of the same real-time FTIR instrument, since full FTIR spectra are collected and for each functional group specific bands can be assigned. The maximum polymerization rate, R_p, in the straight-line region of the sigmoid curve can be determined using the steady-state equation

$$R_p\,(\%\ s^{-1}) = \frac{C_2 - C_1}{t_2 - t_1} \times 100\%$$

Description Peak Fitted Deconvolution.[14] The univariate method is limited when different functional group specific bands overlap each other. Peak fitted deconvolution is another conventional data analysis technique which is very useful if there are no isolated bands available in the FTIR spectrum that can be used for the univariate method. Peak fitted deconvolution can resolve overlapping bands in the FTIR spectra. Vibrational bands have a Lorenz shape when the molecule is not influenced by its surrounding. This is more or less only the case in the gas phase. Since the formulations are liquids, the vibrational bands will be Gaussian broadened. Therefore, after a baseline correction the overlapping bands are calculated by fitting Gaussian curves expressed as

$$Y = a\mathrm{e}^{-[(x-p)/w]^2}$$

However, the selection of the number of bands, their exact position, p, peak height, a, and width, w, are subjective, and therefore prior knowledge, especially of the exact peak position, is required. The band parameters are usually determined out of the IR spectra of the pure components. These parameters are fixed, and Gaussian curves are fitted in the baseline-corrected FTIR. The optimized fit is based on an iterative process in order to reduce the least-squares residuals between the band contour and the sum of the individual peak profiles to a minimum.

Description of SIMPLISMA.[15] The SIMPLISMA approach (simple-to-use interactive self-modeling mixture analysis) is a tool for self-modeling mixture analysis, which means that it resolves mixture data into pure component spectra and concentrations, without using prior information about the mixtures. To show the principle of the SIMPLISMA method, the pure variable concept needs to be introduced. A pure variable is based on the variable with the maximum ratio of the standard deviation to the mean. This ratio is called the purity and is given by the following expression:

$$p_{i1} = \frac{\sigma_i}{\mu_i + \alpha}$$

In this expression, p_{i1} represents the first purity values for all the variables. Assuming that there are pure variables present in the data set, the first pure variable of a data set can be found by taking the variable which has the maximum value p_{i1}. μ_i and σ_i represent the mean and standard deviation of variable i. The constant α is added to the denominator to give variables with a low mean value (i.e., in the noise range) a lower purity value p_{ij}. The effect of the first pure variable needs to be eliminated in order to find the next pure variable. A rationalization of the procedure is as follows. The correlation coefficient r of each variable with the pure variable is calculated. For variables around the pure variable the correlation coefficient r will be high. For variables not related to the pure variable the correlations will be lower. Next, all variables are multiplied by the factor $(1 - r)$. The values of variables correlated with the pure variable will be low, and the values for the variables not correlated with the pure variable will be high. This effectively eliminates all the variables that are correlated with the first pure variable. The maximum in this corrected purity curve now is the second pure variable, and the process can be started all over again. In practice, a determinant-based function is used to correct for pure variables, but the correlation coefficient as explained above is a good analogue.

Now that the pure components have been determined, the original data set can be resolved into pure components and their contributions in the original spectra. The contributions of the pure components in the original spectra can be resolved by a least-squares method.

Description Multivariate Curve Resolution (MCR).[16,17] The spectrum of a multicomponent system, D, can be considered as the sum of individual spectra of its components:

$$D = \sum_{k=1}^{p} S_k C_k$$

where p is number of components that contribute to the observed spectral intensities in D. S_k and C_k are the spectrum of component k and its concentration, respectively. The entire spectroscopic data set of n spectra can be expressed in a matrix, D, of dimension m by n, namely

$$D_{ij} = \sum_{k=1}^{p} S_{ik} C_{jk} \quad \text{for } i = 1, 2, \ldots, m \text{ and } j = 1, 2, \ldots, n$$

The objective of the analysis is to solve the above equation for S and C. There are many different methods to generate the matrices, S, of the spectra of chemical components, and C, of the associated intensities or concentrations. There may be other factors that represent the spectral baseline and other fixed pattern errors from the measurement of the spectra. Therefore, the observed data matrix, D, can be approximated by the matrix product S and C with the first q components and a residue matrix, E, representing experimental errors:

$$D_{m\times n} = S_{m\times q} C_{q\times n} + E_{m\times n}$$

Alternating least-squares regression methods are used to refine the C and S matrices to real spectra and concentration profiles of pure chemical species. This is an iterative process by minimizing the residue matrix, E, while applying some physically meaningful constraints such as the nonnegativity constraint for most spectroscopic data.

Comparison of SIMPLISMA and MCR. Both algorithms SIMPLISMA and MCR are developed to resolve mixture data into pure component spectra and concentrations. With respect to ease of handling the SIMPLISMA method is preferred above MCR. As already mentioned, SIMPLISMA does not need any prior information or adding of constraints to resolve the mixture data. This in contrast to MCR, where prior information either estimates of the pure component spectra or of the concentration profiles must be put into the model to obtain a result at all. Furthermore, the results of MCR will improved significantly if constraints are added to the model. For more complex mixtures MCR is to be preferred above SIMPLISMA. In recent studies of rather complex mixtures the output of SIMPLISMA is used as initial estimates of the pure component spectra for MCR. On the other hand, MCR needs some advanced knowledge of data analysis techniques to use it in an optimal way, but this is largely compensated by its more powerful ability to solve complex time-resolved spectral data.

So with respect to spectral resolving power and reliability the order is MCR > SIMPLISMA > peak fitted deconvolution > univariate method. However, considering the ease of use the reverse order is obtained.

Description of 2D Correlation Spectroscopy. The basic algorithm for the determination of 2D correlation spectra has been developed by Noda.[18] The IR data evaluation is based on the Hilbert transform (HT) of the dynamic intensity changes. The HT algorithm is in matrix notation as follows:

$$\Phi(\nu_1,\nu_2) = \frac{1}{m-1}\tilde{y}(\nu_1)^T \tilde{y}(\nu_2)$$

$$\Psi(\nu_1,\nu_2) = \frac{1}{m-1}\tilde{y}(\nu_1)^T N \tilde{y}(\nu_2)$$

in which $\tilde{y}$ = dynamic spectrum at wavelength υ, m = number of objects (samples), and N = the Hilbert−Noda transformation matrix:

$$N_{jk} = \begin{cases} 0 & j = k \\ 1/\pi(k-j) & j \neq k \end{cases}$$

in which the following matrix is operational

$$N = \frac{1}{\pi}\begin{bmatrix} 0 & 1 & {}^1/_2 & {}^1/_3 & \ldots \\ -1 & 0 & 1 & {}^1/_2 & \ldots \\ -{}^1/_2 & -1 & 0 & 1 & \ldots \\ -{}^1/_3 & -{}^1/_2 & -1 & 0 & \ldots \\ \ldots & \ldots & \ldots & \ldots & \ldots \end{bmatrix}$$

This analysis results is two 2D correlation spectra: $\Phi(\nu_1,\nu_2)$ is the synchronous spectrum and $\Psi(\nu_1,\nu_2)$ the asynchronous spectrum. The synchronous 2D correlation spectrum represents coupled or related changes in the spectral intensity at the two correlated wavenumbers ν_1 and ν_2, while the asyn-

Table 2. Reactivity Ratios As Determined with RT-IR Employing Various Methods[a]

		Kelen−Tudos		extended Kelen−Tudos		NLLS		final values	
M_1	M_2	r_1	r_2	r_1	r_2	r_1	r_2	r_1	r_2
Fum	VE	0.002	0.003	0.00	−0.01	−0.09	−0.01	0	0
Mal	VE	0.007	0.00	0.01	0.00	0.09	−0.01	0	0
Fum	AE	0.07	−0.1	0.00	0.02	−0.1	0.1	0	0
Mal	AE	0.05	−0.01	0.01	0.01	−0.01	0.00	0	0
Fum	HEMA	0.01	1.3	0.02	1.3	0.07	1.4	0	1.3
Fum	EHMA	0.02	1.3	0.02	1.4	0.1	1.3	0	1.3
Fum	HEA	X	X	X	X	X	X	0	>50
HEMA	VE	na	na	16	0	na	na	16	0
HEMA	AE	X	X	X	X	X	X	>100	0
HEMA	HEA	2	0.17	2.1	0.17	1.6	0.15	1.6	0.15
HEMA	NVC	7.2	0.02	7.1	0.1	7.3	0.01	7.3	0.01
HEA	NVC	1.4	0.2	1.5	0.2	1.3	0.1	1.3	0.01

[a] Fum = dibutyl fumarate; Mal = dibutyl maleate; HEMA = hydroxyethyl methacrylate; HEA = hydroxyethyl acrylate; VE = hydroxyethyl vinyl ether; AE = hydroxyethyl allyl ether; EHMA = ethyl-α-hydroxy methacrylate; NVC = *N*-vinylcaprolactam; X = unable to determine; NA = not applicable.

chronous correlation spectrum represents independent or separate variations.

Determining Reactivity Ratios. The copolymerization reactivity ratios were determined using Kelen−Tudos, extended Kelen−Tudos, and the more recently described nonlinear least-squares (NLLS) methodology[20] employing multiple feed ratios. The so-obtained reactivity ratios were used in a feed−polymer composition plot in order to validate the determined reactivity ratios. Only the reactivity ratios best describing the copolymerization based on the feed−polymer composition plot are reported. In one case, i.e., hydroxyethyl acrylate−*N*-vinylcaprolactam yielded the NLLS method, not the reactivity ratios describing the feed−polymer composition. However, still the result obtained with the NLLS method was closest to the real value. As control, time−conversion profiles were converted into a monomer feed−polymer composition profile and compared with the profiles based on the determined reactivity ratios. All copolymerizations were assumed to proceed according to the ultimate model.[21] Further kinetic analysis was performed as initially described by Decker.[11a]

Results and Discussion

Determination of Reactivity Ratios. a. Dibutyl Fumarate−Hydroxyethyl Vinyl Ether and Dibutyl Maleate−Hydroxyethyl Vinyl Ether Systems. The fumarate−vinyl ether mixture and the maleate−vinyl ether systems are the systems which have been studied by Decker[11a] before. We investigated these mixtures in order to validate our methodology for determination of the reactivity ratios. The maleate−vinyl ether system behaved as described before, and similar to Decker we found reactivity ratios for dibutyl maleate−hydroxyethyl vinyl ether, $r_1 = 0$, $r_2 = 0$ (see Table 2). The fumarate−vinyl ether system could not be analyzed in the same way as Decker has previously reported. To our initial surprise the fumarate isomerizes upon irradiation partly into the corresponding maleate, as indicated by the appearance of a maleate absorption at 1406 cm^{-1}. This process is photoinduced, not radical induced, and we confirmed the formation of dibutyl maleate by irradiation of dibutyl fumarate with a Fusion F600D bulb (dose 2 J/cm^2) and the analysis of this mixture with ^1H and ^{13}C NMR. Upon prolonged irradiation at room temperature almost complete conversion into the maleate could be achieved (>10 J/cm^2). Consequently, the fumarate consumption in the IR spectra had to be corrected for the maleate formation.[23] A representative graph of the time−conversion plot is shown in Figure 1, in which the maleate formation is represented by a negative conversion. The fact that this isomerization was unnoted previously can be explained by the fact that only a single absorption was monitored instead of the full IR spectrum. On the basis of solely monitoring the fumarate bond in a fumarate−vinyl ether system, it was previously concluded that the fumarate was more reactive compared to the maleate in a maleate−vinyl ether system.[11] However, using corrected fumarate conversions, we observed comparable rates of copolymerizations for both systems.

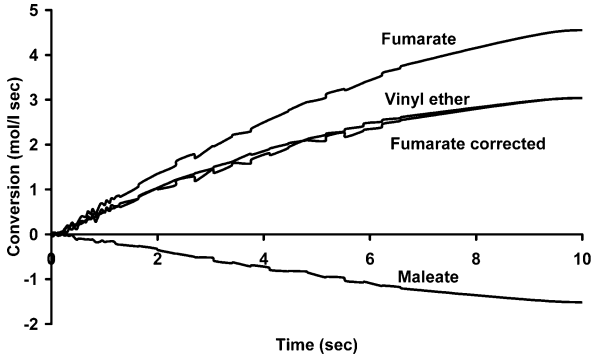

Figure 1. Time−conversion profile of a fumarate−vinyl ether mixture as determined with RT-FTIR under nitrogen.

Scheme 1. Possible Mechanisms via Which a Fumarate−Vinyl Ether (Fum−VE) Copolymerization Yields Perfect Alternating Polymers

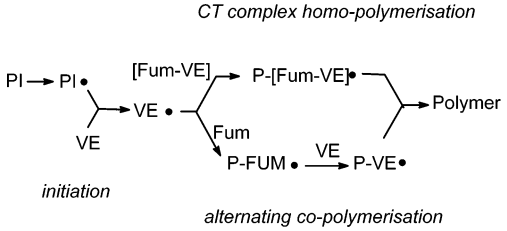

Still we obtained a similar result, and the reactivity ratios for dibutyl fumarate−hydroxyethyl vinyl ether mixtures are $r_1 = 0$, $r_2 = 0$. Identical values were found for the maleate−vinyl ether system.[24]

These perfect alternating copolymerizations can proceed via two different mechanistic pathways, as depicted in Scheme 1. It can be regarded as homopolymerization of a charge-transfer complex or be regarded as alternating copolymerization. In both cases it is likely that the radical which starts the polymerization is formed via the addition of a photoinitiator radical to a vinyl ether double bonds due to the steric effects which play a pivotal role in radical additions.[25]

Following the kinetic analysis with respect to the rate of polymerization, i.e., $R_p = K\{[M_1][M_2]\}^{1/2}$ for an alternating copolymerization and $R_p = K[M_1][M_2]$ for the homopolymerization of a charge-transfer complex, we found identical results as previously determined by Decker. Both polymerizations can best be described as homopolymerizations of a charge-transfer complex.[26] The similar results indicate that the analyzing methodology using RT-FTIR instead of RT-IR can be considered to be correct. As the double bond absorptions are well resolved only this method has been used for the data analysis.

b. Dibutyl Fumarate−Hydroxyethyl Allyl Ether and Dibutyl Maleate−Hydroxyethyl Allyl Ether Systems. Considering the reactivity ratios found, both r_1 and r_2 are 0; it is tempting to assume that these mixtures will react in a similar fashion compared to the blends with vinyl ethers. Comparing the observed reactivity ratios with the values in the literature ($r_1 = 1$, $r_2 = 0$),[27,28] some homopolymerization of the fumarate might be assumed under these conditions. However, in these peroxide-initiated copolymerizations the excess of fumarate was incorporated via a degradative chain transfer reaction, and therefore a value of $r_1 > 0$ was found.[28] The kinetic analysis described above revealed that these polymerizations are not homopolymerizations of a charge-transfer complex under photoinitiated conditions, but are alternating copolymerizations formed via a cross-propagation mechanism. Again well-resolved double bond signals were found.

c. Dibutyl Fumarate−Hydroxyethyl Methacrylate and Dibutyl Fumarate−Ethyl α-Hydroxymethacrylate Systems. Hydroxyethyl methacrylate (HEMA) and ethyl-α-hydroxy methacrylate (EHMA) can be considered structural isomers; only the position of the hydroxy functionality differs. It has been well established that α-hydroxy or alkoxy methacrylates can be regarded as methacrylates with an increased reactivity of the double bond, i.e., in homopolymerizations higher rates are observed for ethyl-α-hydroxy methacrylate derivatives compared to those of hydroxyethyl methacrylate derivatives,[30] although a direct comparison between the two isomers (HEMA vs EHMA) is lacking. In case this positional change of the hydroxy functionality would have a large effect on the electronic nature on the polymerizing double bond; then it is expected that also the reactivity ratios would be different. However, in case these effects are only minor, similar reactivity ratios in their copolymerizations could be expected. As expected, on the basis of the available literature of EHMA derivatives, EHMA exhibited a higher maximum rate of homopolymerization (0.25 mol/(L s)) compared to HEMA (0.17 mol/(L s)). In copolymerizations also an increased polymerization rate was found (maximum rates of poymerization 1:1 molar mixture dibutyl fumarate/EHMA: 0.12 mol/(L s); 1:1 molar mixture dibutyl fumarate/HEMA 0.08 mol/(L s)).

Surprisingly, despite the differences in copolymerization rates, the same reactivity ratios ($r_1 = 0$ and $r_2 = 1.3$) were found for both types of methacrylates.[31] This suggest that this variation in hydroxy attachment has only a minor effect on the electronic nature of the reactive double bond although the effect is large enough to have a pronounced effect on the rates of polymerization, indicating that the origin of this reactivity difference is probably due to reduced termination. Again well-resolved double bond IR absorptions are observed.

d. Dibutyl Fumarate−Hydroxyethyl Acrylate Systems. We were unable to determine the reactivity ratios of these mixtures as we could not determine the fumarate conversion in a reliable manner due to strong overlapping peaks. Assuming no isomerization of fumarate to maleate occurs, still the decrease in fumarate double bond absorption was 5% at most. Besides, most of this fumarate conversion took place when hydroxyethyl acrylate (HEA) was already for approximately 95% polymerized. During the homopolymerization of the bulk of the acrylate, in the various mixtures, we could not detect any fumarate consumption (within the error of measurement). Kinetically, however, the amount of fumarate had a severe impact on the rate of polymerization as the hydroxyethyl acrylate polymerization is strongly retarded by the addition of dibutyl fumarate. Consequently, some copolymerization must occur under these conditions, and we estimate the following reactivity ratios $r_1 = 0$ and $r_2 > 50$, which can be considered to be an educated guess.

e. Hydroxyethyl Methacrylate−Hydroxyethyl Vinyl Ether Systems. The amount of methacrylate conversion exceeded 15% before a reliable significant amount of vinyl ether conversion could be observed. Therefore, for the determination of the reactivity ratios only the extended Kelen−Tudos methodology could be used since this allows the determination of reactivity ratios at higher conversion levels. A disadvantage is that the reactivity ratios determined via this method are considered less accurate compared to the other methods like Kelen−Tudos or the NLLS method. The following reactivity ratios were found: $r_1 = 16$ and $r_2 = 0$, which are in line with the literature values.[32]

f. Hydroxyethyl Methacrylate−Hydroxyethyl Allyl Ether Systems. In these photoinitiated copolymerizations we were unable to detect any allyl ether conversion. In fact, taking the dilution factor into account, no influence of the allyl ether on the rates of polymerization could be found as well. Kinetically only a methacrylate homopolymerization was observed and no copolymerization. Therefore, with respect to the reactivity ratios we suggest $r_1 > 100$ and $r_2 = 0$, which is in line with the values ($r_1 = 99-107$, $r_2 = 0$) observed in the literature.[27]

g. Hydroxyethyl Methacrylate−Hydroxyethyl Acrylate Systems. In all the above-mentioned copolymerizations we were able to find well-resolved absorptions from the polymerizing double bonds. Although hydroxyethyl acrylate (HEA) is far more reactive in a homopolymerization compared to hydroxyethyl methacrylate (HEMA), the reported reactivity ratios of these systems suggest that this is not the case for these mixtures.[33] Unfortunately, none of the IR absorptions from the reactive double bond, being around 3100, 1640, or 810 cm^{-1}, are well resolved. In fact, generally a single peak is observed around 810 cm^{-1}, as is illustrated by the 3D time−conversion plot shown in Figure 2.

Therefore, this copolymerization serves as an ideal test case for the reliability of the different methods for data treatments/analysis. It should be explicitly noted that the same data set was used in all cases, which is inherently multivariate (time × wavelength × absorption). Only the mathematical treatment of the raw data differs.

Comparison of Analytical Methods. a. Other Well-Resolved Absorptions. Taking the IR spectra of the pure monomers into account, it is safe to assume

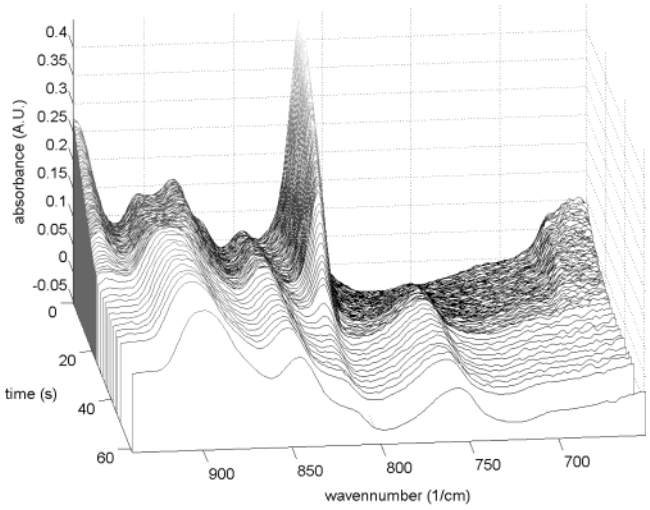

Figure 2. 3D RT-FTIR plot of a HEMA−HEA (1:1 molar mixture) copolymerization.

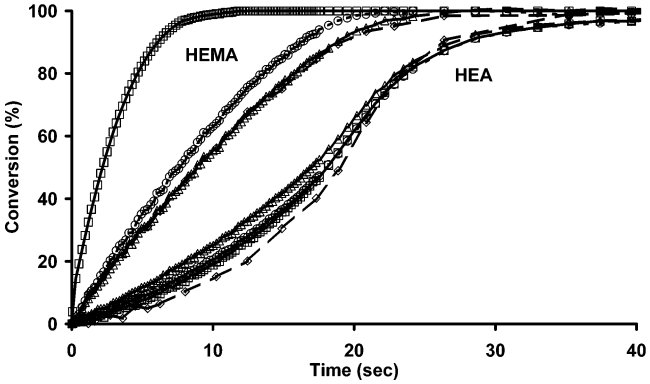

Figure 3. Time−conversion profiles of a 1:1 HEMA−HEA molar mixture as obtained by various data treatments: univariate method (squares); deconvolution (diamonds); SIMPLISMA (triangles); multivariate curve resolution (circles).

that the IR absorption at 940 cm^{-1} can be attributed to HEMA while the IR absorption at 988 cm^{-1} can be attributed to HEA. A possible source of errors employing this methodology is that underlying IR absorptions with respect to the frequencies studied are not noticed. Moreover, although generally true, an assumption is that although the vibration does not originate from the reacting double bond; still its decrease can be linearly related to the reactive double bond. In Figure 3 the results of this analysis, in terms of a polymerization profile, of a 1 to 1 molar HEMA/HEA mixture are shown together with the results from the other data analysis.

b. Peak Fitted Deconvolution. Deconvolution of peaks is frequently used for the separation into the individual components. In Figure 4 the IR absorptions of both monomers as well as the 1:1 molar mixture are shown.

Clearly the IR vibration at 812 cm^{-1} of the mixture could consist out of two bands. Assuming that the IR vibrations are not changed in a different environment, the monomer frequencies, i.e., for HEMA 815 cm^{-1} and for HEA 810 cm^{-1}, can be used as positions of the peak frequencies of the individual components. IR vibrations possess in the gas phase a Lorentzian shape, but in the liquid phase a Gaussian line broadening is observed. As a consequence, it is assumed that Gaussian curve fitting can be used in the deconvolution method. A further disadvantage of this method is that it performs

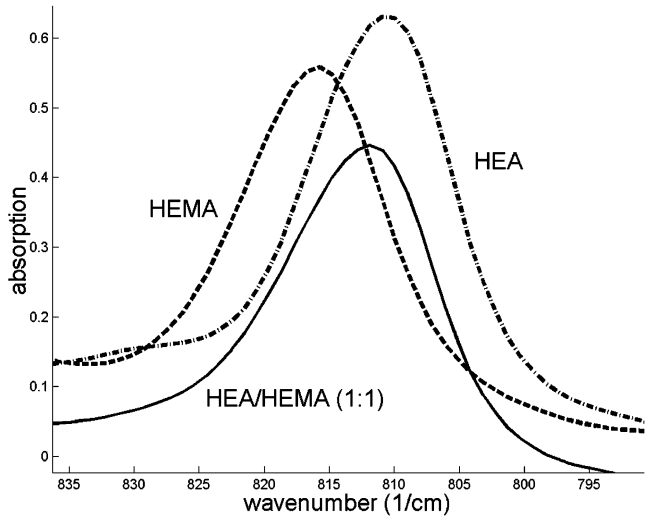

Figure 4. Measured IR spectra of pure HEA, HEMA, and the 1:1 molar mixture of HEMA and HEA.

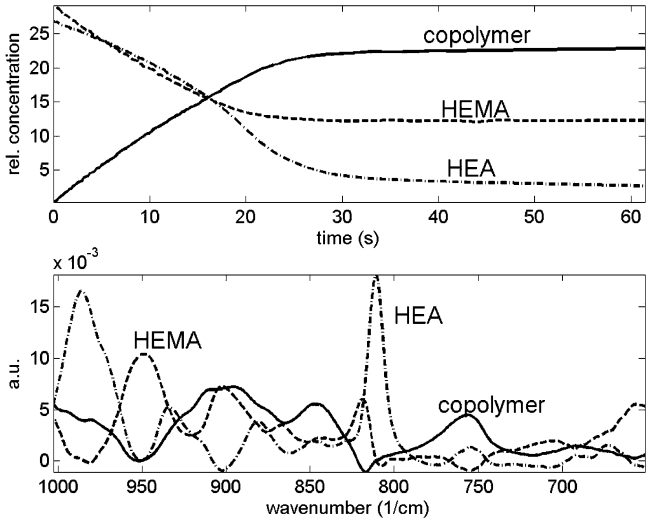

Figure 5. SIMPLISMA spectrum of the copolymerizing 1:1 molar HEMA−HEA mixture.

best if both IR vibrations possess almost the same extinction coefficient. Unfortunately, the extinction coefficient of HEMA is only a fifth of the extinction coefficient of HEA, and this can be another source of errors.

c. SIMPLISMA Method. The results of the SIMPLISMA calculations are shown in Figure 5. The raw data could be reconstructed by calculating three pure variables. This results in three pure spectra and three concentration profiles of the resolved components: two decreasing concentration profiles of the monomers HEA and HEMA and one increasing profile of the copolymer. The calculated pure spectra of HEA and HEMA are in good agreement with the measured pure spectra (see Figure 6). Comparison of the measured pure spectra with the calculated pure spectra of the components is an objective method to examine the quality of the calculations.

In the spectral region of 820−800 cm^{-1} of Figure 5 HEA and HEMA show two separated peaks. One should be aware that the contributions of the pure components are resolved by fitting the pure spectra with the original spectra with a least-squares method and are thus not based on just one peak in the spectrum, as is the case with classical methods like peak deconvolution. The

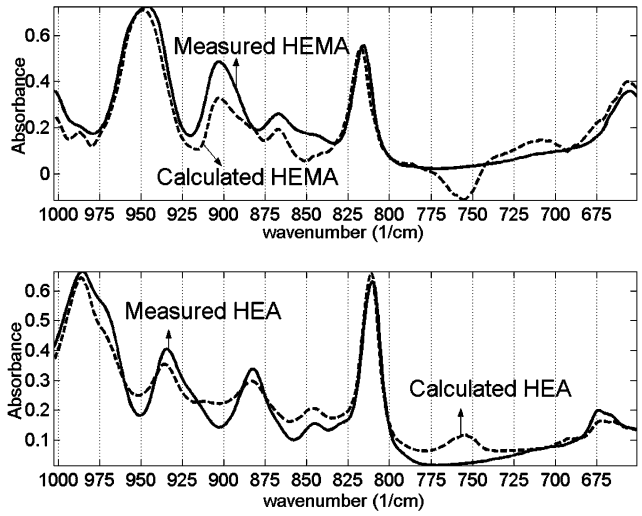

Figure 6. Comparison of the measured spectra and calculated spectra of HEA and HEMA with the SIMPLISMA method.

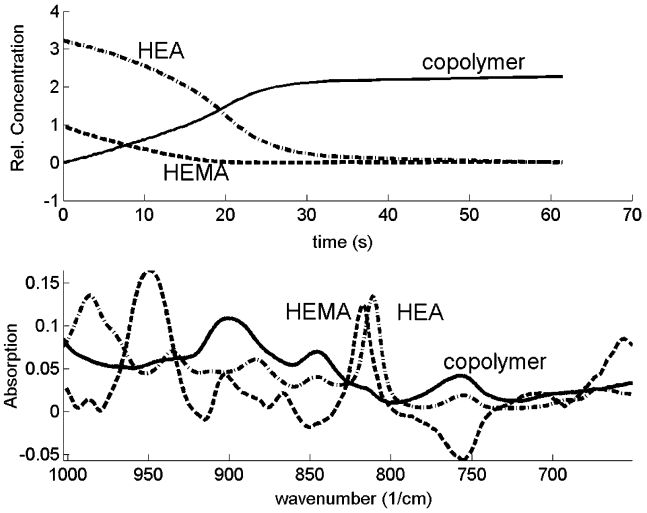

Figure 7. Multivariate curve resolution spectrum of the copolymerizing 1:1 molar HEMA−HEA mixture.

concentrations of monomer and polymer can be derived from their relative concentrations (based on absorbance) and their relative extinction coefficients. The calculated concentrations of HEA and HEMA can then be transferred in polymerization profiles as is shown in Figure 3.

d. Multivariate Curve Resolution. Again, three resolved pure spectra and three concentration profiles could reconstruct the raw spectral data. Comparison of the pure spectra (Figure 7) shows that they are in good agreement with the measured pure spectra and the calculated pure spectra by SIMPLISMA. The differences between the results obtained by SIMPLISMA and MCR are very small. For the present case at hand, that is, a somewhat uncomplicated time evolving data set, it is advised to use the SIMPLISMA software because it is a simple to use interactive data analysis tool. It is not a prerequisite to have any knowledge of complex data analysis methods, and it is intended for users who are familiar with spectra interpretation. On the other hand, MCR needs some advanced knowledge of data analysis techniques to use it in an optimal way, but this is largely compensated by its more powerful ability to solve complex time-resolved spectral data.

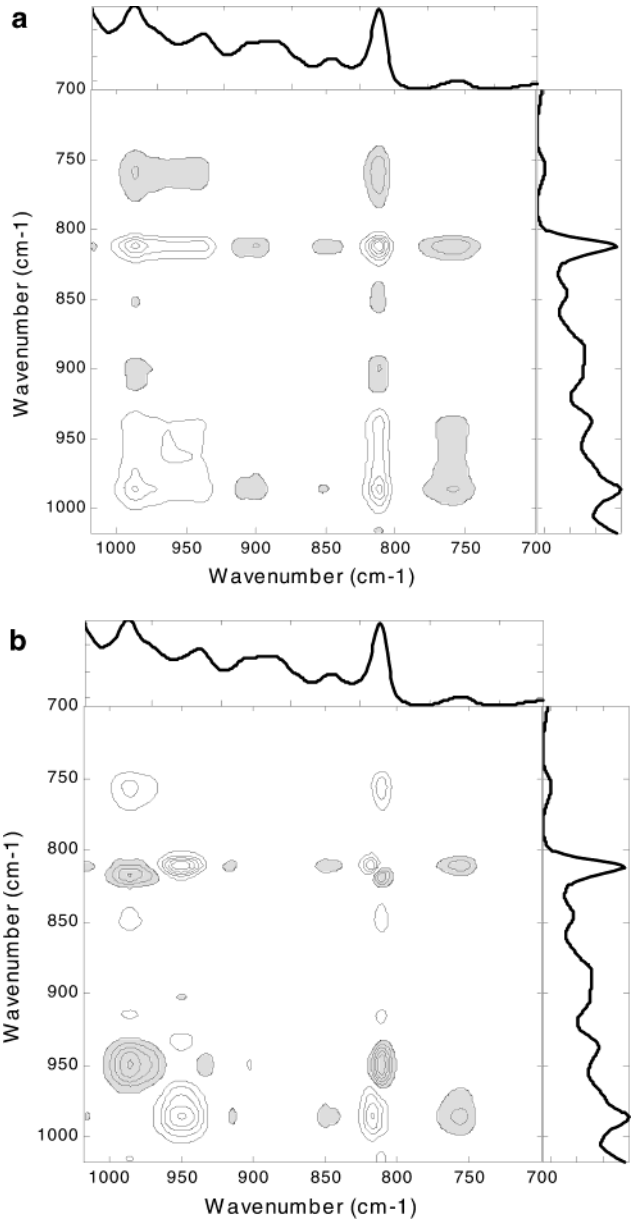

Figure 8. (a) Synchronous Hilbert transform 2D correlation spectrum and (b) asynchronous Hilbert transform 2D correlation spectrum of the copolymerizing 1:1 molar HEMA−HEA mixture.

e. Using 2D Correlation Spectroscopy. A peak model based deconvolution method as previously described can intrinsically give the wrong results. A small shift in IR frequency from one of the components can result in a wrong peak assignment. Moreover, IR vibrations tend to shift due to environmental changes. So the use of the IR frequencies of the monomers can be questionable. It can even be that the peaks are shifted as such that the 812 cm^{-1} is the position of both absorptions in the mixture and not a combined convoluted peak. Employing 2D correlation using the Hilbert transform can solve these analytical problems. This methodology of data processing results in a so-called synchronous and an asynchronous spectrum as shown in Figure 8a,b for the 750−1000 cm^{-1} spectral region.

The interpretation of these spectra starts with the relative simple synchronous spectrum (Figure 8a). Three autopeaks are visible and a few positive and negative cross-peaks. Peaks that are in the same phase undergo

Table 3. Sequence of Spectral Intensities According to the Hilbert Transform Scheme Titels

ν_1 (cm^{-1})	ν_2 (cm^{-1})	$\Phi(\nu_1,\nu_2)$	$\Psi(\nu_1,\nu_2)$	sequence	
988	940	+	−	ν_1 after ν_2	HEA after HEMA
	816	+	−	ν_1 after ν_2	HEA after HEMA
	760	-	+	ν_1 after ν_2	HEA after polymer
940	811	+	+	ν_1 before ν_2	HEMA before HEA
845	811	−	−	ν_1 before ν_2	polymer before HEA
816	811	+	+	ν_1 before ν_2	HEMA before HEA
811	760	-	+	ν_1 after ν_2	HEA after polymer

the same change, for instance, considering a trace at 812 cm^{-1} (the reactive double bonds of the monomers). The peaks at 812, 950, and 980 cm^{-1} have the same phase, and they all reduce in time. The peaks at 760, 850, and 910 cm^{-1} possess an opposite phase, and they all increase in time, which means they originate from the formed polymer. This information can be obtained as well from the univariate IR analysis.

The real strength of this analysis tool lies in the asynchronous spectrum (Figure 8b). All the cross-peaks are now resolved into two separate peaks. The peak at 812 cm^{-1} is now separated into two distinct asynchronous correlations. The peak at 816 cm^{-1} is positively correlated with the peak at 811 cm^{-1}. Bearing in mind that the autopeak at 812 cm^{-1} was positive in the synchronous spectrum, it can be shown by following the analysis as described by Noda[18] that the peak at 816 cm^{-1} decreases first followed by the absorption at 811 cm^{-1}. This procedure is repeated for the full IR spectra (see Table 3), in which the signs in both the synchronous and the asynchronous spectra are taken into account; it is clear that HEMA reacts predominantly first followed by the HEA polymerization. Surprisingly it seems that the polymer absorption at 760 cm^{-1} appears to originate from HEMA containing polymer only as it is mainly formed during the methacrylate polymerization.

It should be explicitly noted that based on this analysis there is a small shift in the spectral frequencies observed for the mixture. For a correct deconvolution procedure the absorption at 816 cm^{-1} instead of 815 cm^{-1} for HEMA has been used and 811 cm^{-1} instead of 810 cm^{-1} for HEA. Although at first glance this difference might seem small, it is large enough to yield erroneous time−conversion profiles.

f. Comparing the Techniques. Using different feed compositions, the following reactivity ratios were determined, $r_1 = 1.6$ and $r_2 = 0.15$ (see below), which were applied in the determination of the "theoretical" relation between the feed composition and the polymer composition. Next the time−conversion profiles obtained via the different methods of a 50:50 HEMA:HEA mixture were converted into the corresponding feed−polymer composition profile. The results are shown in Figure 9. It can clearly be seen from Figure 9 that the results based on the simple univariate method fails as a large deviation between the "theoretical" feed−polymer composition (Figure 9, solid line) and the determined relation according to the univariate method (Figure 9, squares). Still, in principle, if the correct frequency has been chosen, the univariate method should give a result similar to the theoretical relation. The only HEMA absorption which we could find, being convinced that it was only HEMA absorption, was at 645 cm^{-1}. A direct consequence of the very low intensity of this signal is that the time−conversion profile contains much noise. In fact, because of this high noise level this absorption

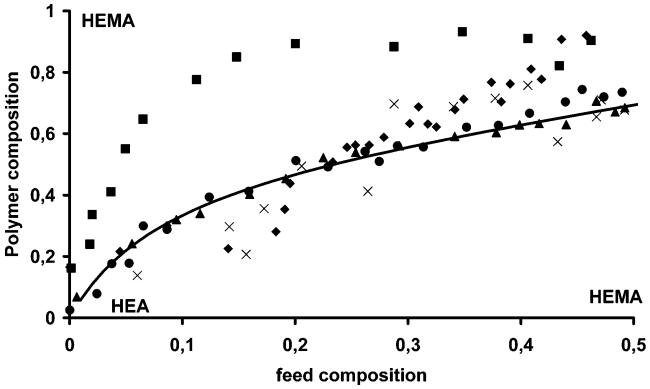

Figure 9. Comparison of the different analytical techniques using the monomer feed−polymer composition relation: solid line theoretical curve based on $r_1 = 1.6$, $r_2 = 0.15$; univariate method at 939 and 985 cm^{-1} (squares); deconvolution (diamonds); SIMPLISMA (triangles) multivariate curve resolution (circles) and univariate method at 645 and 985 cm^{-1} (crosses).

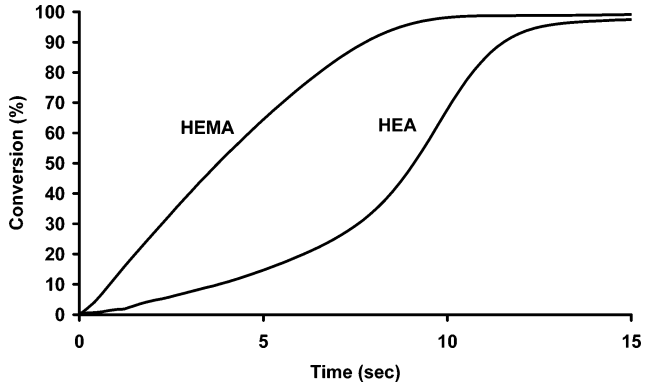

Figure 10. Time−conversion profile of a 20:80 molar HEMA−HEA mixture as determined with RT-FTIR under nitrogen.

is normally unusable. But after performing twice a noise reduction procedure, we had smoothed the data sufficiently to be able to calculate the feed−polymer composition relation ship as is shown in Figure 9 (crosses). Indeed, it can be stated that the result is now appears to be in agreement with the theoretical relation taking a large error bar into account.

The relation as obtained from the deconvolution method (Figure 9, diamonds) could be regarded as following the theoretical relation if one considers a large error bar as well. Both the SIMPLISMA (triangles) and MCR (circles) methods yield a feed−polymer composition relation, which is identical to the "theoretical" relationship. So regarding the reliability of the obtained data, only the two multivariate methods, i.e., SIMPLISMA and MCR, give good results with respect to the feed−polymer composition profile.

g. HEMA/HEA Reactivity Ratios. Combining all the analytical data for these HEMA/HEA mixtures and evaluating them, the following reactivity ratios were found: $r_1 = 1.6$ and $r_2 = 0.15$.[27,33] In this copolymerization the initial rates are dominated by the methacrylate and not by the acrylate and the composition of the polymer will drift severely as is illustrated by the time−conversion profile of a 20:80 HEMA:HEA mixture shown in Figure 10. This figure clearly shows that the faster acrylate homopolymerization only takes place after full methacrylate conversion. Moreover, up to 90 mol % HEA in the copolymerizing mixture, the maximum rate of the HEMA consumption remains unaffected by changes in the HEA concentration. This indicates nicely that the

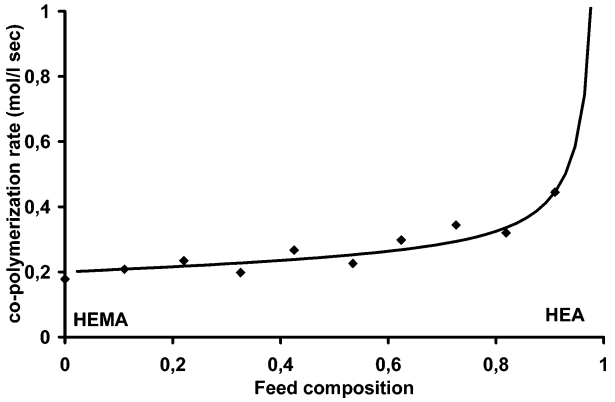

Figure 11. Monomer feed−maximum rate of copolymerization relation for HEMA−HEA mixtures.

methacrylate dominates the copolymerization and that a severe composition drift takes place.

Kinetically the maximum rates of copolymerization, as determined with IR, can be linked to the monomer feed compositions according to the following formulas:[34]

$$R_p = \frac{r_1[M_1]^2 + 2[M_1][M_2] + r_2[M_2]^2}{(r_1^2\delta_1^2[M_1]^2 + 2\Phi r_1 r_2[M_1][M_2] + r_2^2\delta_2^2[M_2]^2)^{1/2}} Ri^{0.5}$$

in which R_p is the rate of polymerization, r_1 and r_2 are the copolymerization ratios, $[M_1]$ and $[M_2]$ are the concentration of monomers 1 and 2, respectively, δ_1 and δ_2 are the termination constants for M_1 and M_2, respectively, and Φ is the cross-termination constant. As the reactivity ratios are known, δ_1 and δ_2 determined from the homopolymerization of both monomers only Φ remains an unknown in this rate equation. Using multiple feed compositions, a value for $\Phi = 2$ was determined, and the copolymerization rate−monomer feed composition relation ship is shown in Figure 11.

So the HEMA/HEA copolymerization as studied with RT-FTIR is a textbook example of composition drift in which all the copolymerization equations apply.

h. Hydroxyethyl Methacrylate Copolymerization with *N*-Vinylcaprolactam. Vinyl amides like *N*-vinylcaprolactam, *N*-vinylpyrrolidone, and *N*-vinylformamide and its derivatives are more prone to copolymerize than vinyl ethers. This is illustrated by the reactivity ratios $r_1 = 7.3$ and $r_2 = 0.01$ as well as the higher rates of polymerization compared to those of the HEMA−vinyl ether mixtures. Although this system has not been evaluated in the literature, the values are in accordance with the ratios for a methyl methacrylate−*N*-vinylpyrrolidone mixture.[35]

i. Hydroxyethyl Acrylate Copolymerization with *N*-Vinylcaprolactam. *N*-Vinylcaprolactam and *N*-vinylpyrrolidone are frequently added to acrylates in order to increase the rate of polymerization in acrylate-based formulations and also to reduce the oxygen sensitivity of the acrylate polymerizations.[36] The reasons for these increased rates of copolymerization are still unknown, especially since the increased rates were observed with photo-DSC, and consequently the reactivity ratios were not determined previously. However, using IR spectroscopy, the monomer absorptions involved appear to be well resolved and the reactivity ratios can be determined relatively easily. Employing all methods for the determination of the reactivity ratios $r_1 = 1.3$ and $r_2 = 0.1$ were found. These values were validated employing the monomer feed−polymer composition relation. As can be clearly observed in Figure 12, there is a deviation employing these ratios especially in the region containing low amounts of acrylate. The reactivity ratios which correctly described with experimental results of $r_1 = 1.3$ and $r_2 = 0.01$.

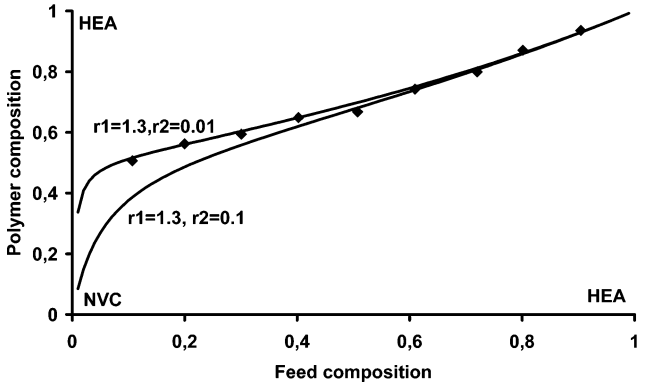

Figure 12. Monomer feed−polymer composition relation for HEA−NVC mixtures.

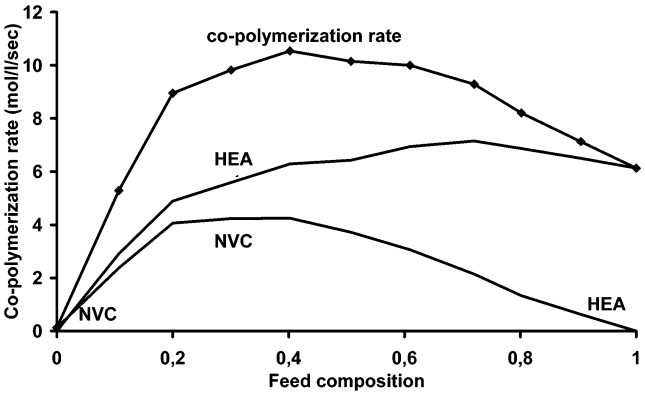

Figure 13. Monomer feed−maximum rate of copolymerization relation for HEA−NVC mixtures.

Regarding the reactivity ratios it can be concluded that the copolymerization is governed by the acrylate. Does this imply that the acrylate-based propagating radical is more stable compared to the NVC-based radical? Considering the rates for the homopolymerizations, one is tempted to conclude the opposite as the HEA homopolymerization proceeds 60 times faster than the NVC homopolymerization (rates 6.1 mol/(L s) vs 0.12 mol/(L s)). In the HEMA/HEA example it was the slower homopolymerizing double bond which dictated the polymerization. In Figure 13 the copolymerization rates vs the feed composition are shown.

On the basis of the copolymerization equations, the highest observed rate in case both $r_1 > 0$ and $r_2 > 0$ is one of the monomers. Consequently, the highest observed copolymerization rate should, in this case, be the acrylate homopolymerization rate. From Figure 8 it is evident that this is not the case as the highest rates are observed around the 1:1 molar mixture (10.6 mol/(L s)), which means that the copolymerization equations with respect to the rate do not apply in this case. However, it should be noted that the copolymerization proceeds not in a 1:1 fashion which is illustrated by the fact that in the case of the 1:1 molar feed ratio still 30% of the NVC has not reacted when all the acrylates have been consumed.

How can such a result be rationalized? A valid explanation might be that besides the two monomers another species is present in the copolymerization. This species should be more reactive compared to both the monomers and should be formed from both monomers. We propose that a charge-transfer complex between the monomers is in fact the third reactive "monomer" and that this copolymerization is best described as a terpolymerization of NVC, HEA, and the NVC−HEA charge-transfer complex. This explanations account for several observations. The fact that the highest rate is observed around the 1:1 molar ratio has become obvious as the highest CT complex concentration is expected around the 1:1 molar ratio. Furthermore, the CT complex copolymerizes with different ratios with the acrylate and NVC; consequently, unequal reactivity ratios are found for the "copolymerization" and NVC remains present at the 1:1 molar mixture (which possess the highest rate). Finally, radical CT polymerizations tend to be less susceptible to oxygen inhibition, which gives an explanation for the reduced oxygen inhibition effect.[36a] Besides the contribution of the CT complex to the increased reactivity, an effect on the rate caused by the polarity on NVC might be expected as well.[37]

As an alternative, it could be that this system should be described as the copolymerization of the CT complex with HEA, and all the above-mentioned observations are in line with this explanation. However, at NVC contents above 60 mol % slightly more NVC is incorporated in the formed polymer then could be expected on the basis of the total available HEA amount. Employing a feed ratio of HEA:NVC = 1:9, 1.3 times the amount of NVC is incorporated than could be expected on the basis of a copolymerization model.

Complete polymerization of both HEA and NVC can be achieved with a monomer mixture containing up to 30% NVC.

Supplement: Homopolymerization of HEA. Most analytical methods for data treatment of the HEMA−HEA mixtures showed minor disturbances near the 812 cm^{-1} frequencies. This was combined with the fact that according to the Hilbert transform the polymer peak at 760 cm^{-1} originates dominantly from the methacrylate and not from the acrylate. Therefore, we wondered whether a polyacrylate absorption could be present around the 812 cm^{-1} frequency. This implies that the standard acrylate peak at 810 cm^{-1}, which is employed in most analysis, is already a convoluted peak. To answer this question, we applied the Hilbert transform to the homopolymerization of HEA, of which the asynchronous spectrum is shown in Figure 14.

We were stunned by the fact that this analysis revealed that indeed the acrylate absorption at 810 cm^{-1} is a convoluted peak. At this position also a polyacrylate absorption occurs, and since most acrylate polymerizations are monitored at this position, this would imply that most of the literature data for acrylates would be erroneous! Fortunately, comparing the time−conversions profiles for the HEA polymerization based on the absorptions at 810, 1410, and 1637 cm^{-1}, they all gave the same result (within the 2% error of measurement). Moreover, the conversions based on the 810 cm^{-1} absorption were in good agreement with the conversions as determined with ^{1}H and ^{13}C NMR (within a 5% error margin). Apparently the extinction coefficient of the polyacrylate peak at this position is small compared to the monomer, and therefore it does not influence the correct determination of acrylate conversion levels. However, the polymer is formed whereas the acrylate is consumed. As a consequence, the Hilbert transform, being sensitive toward phase differences, can clearly distinguish two peaks—one of which the intensity is decreasing and one of which the intensity is increasing. This experiment therefore nicely demonstrates the sensitivity of the Hilbert transform for phase differences in a reacting mixture.

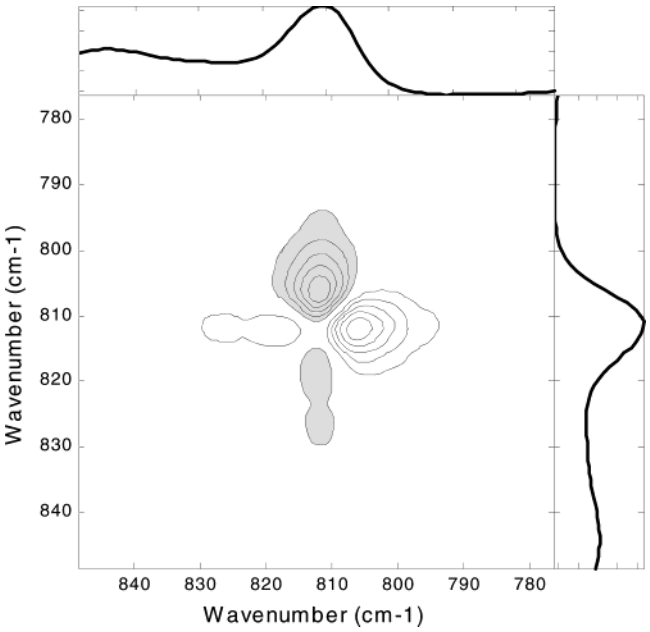

Figure 14. Asynchronous 2D correlation spectrum of the HEA homopolymerization.

Consequently, although the 810 cm^{-1} absorption is a convoluted peak, the deviation in conversion due to the formation of polyacrylate is negligible, and the 810 cm^{-1} absorption can still be employed for the determination of the conversion.

Conclusion

In conclusion, we have demonstrated that RT-FTIR spectroscopy is a facile technique for the determination of copolymerization reactivity ratios, in particular when the dynamic data of this technique are interpreted by advanced multivariate statistical techniques. Besides correct reactivity ratios, also kinetic information regarding the reaction rates of the individual components can be obtained. It has been shown independently (Figure 3 vs Figure 10) for a monomer like HEA, in a HEMA−HEA mixture with its selective IR peaks, that univariate as well multivariate techniques perform in the same way, which suggests to choose the more simple univariate technique as always a first accurate guess. However, in the case of a monomer like HEMA with its interfering IR peaks in the same HEMA−HEA mixture, the multivariate techniques SIMPLISMA, multivariate curve resolution, and 2D correlation spectroscopy clearly outperform the classical univariate calculation methods. The 2D correlation spectroscopy is obviously a powerful tool for the identification of absorptions in complex copolymerizing mixtures. Furthermore, in the case of convoluted peaks only the 2D correlation spectroscopy yields the essential information required for a correct deconvolution of the separate absorptions. By this technique, it was demonstrated that the standard acrylate absorption at 810 cm^{-1}, which is frequently

used in RT-FTIR analysis, is in fact a convoluted peak consisting of the acrylate absorptions and polymer absorption with a small extinction coefficient.

On the basis of these more accurate multivariate reaction profiles, the following chemical conclusions can be drawn: The copolymerization of a fumarate−vinyl ether system should be regarded as a homopolymerization of the charge-transfer complex while in the case of a fumarate−allyl ether system it should be regarded as a perfect alternating copolymerization based on this kinetic evidence. Furthermore, the copolymerization of HEMA with HEA can be considered a textbook example, and all the copolymerization rules apply nicely. The HEA−NVC copolymerization should be regarded as a terpolymerization between HEA, NVC, and the HEA−NVC charge-transfer complex, of which the charge-transfer complex possesses the highest reactivity.

Acknowledgment. The management of DSM Research, DSM Coating Resins, and DSM Desotech are kindly acknowledged for their permission to publish this work.

References and Notes

(1) (a) Nie, J.; Rabek, J. F.; Linden, L.-A. *Polym. Int.* **1999**, *48*, 129. (b) Narayanan, V.; Scranton, A. B. *Trends Polym. Sci.* **1997**, *5*, 415. (c) Lovell, L. G.; Stansburry, J. W.; Syrpes, D. C.; Bowman, C. N. *Macromolecules* **1999**, *32*, 3913 and references therein. (d) Kloosterboer, J. G. *Adv. Polym. Sci.* **1988**, *84*, 1.

(2) (a) Tryson G. R.; Schultz A. R. *J. Polym. Sci., Polym. Phys. Ed.* **1979**, *17*, 2059. (b) Decker, C.; Elzaouk, B.; Decker, D. *J. Macromol. Sci., Pure Appl. Chem.* **1996**, *A33*, 173 and references therein. (c) Doornkamp, A. T.; Tan, Y. Y. *Polym. Commun.* **1990**, *31*, 362. (d) Lecamp, L.; Youssef, B.; Bunel, C.; Lebaudy, P. *Polymer* **1999**, *40*, 1403. (e) Khudyakov, I. V.; Legg, J. C.; Purvis, M. M.; Overton, B. J. *Ind. Eng. Chem. Res.* **1999**, *38*, 3353. (f) Selli, E.; Bellobono, I. R. In *Radiation Curing in Polymer Science and Technology*; Fouassier, J. P., Rabek, J. F., Eds.; Elsevier: London, 1993, Vol. 3, p 1. (g) Decker, C.; Masson, F.; Bianchi, C. *Polym. Prepr.* **2001**, *42*, 304. (h) Yamada, B.; Azukizawa, M.; Yamazoe, H.; Hill, D. J. T.; Pomery, P. J. *Polymer* **2000**, *41*, 5611. (i) Seno, M.; Fukui, T.; Hirano, T.; Sato, T. *J. Polym. Sci., Part A: Polym. Chem.* **2000**, *38*, 4264. (j) Doetschman, D. C.; Mehlenbach, R. C.; Cywar, D. *Macromolecules* **1996**, *29*, 1807.

(3) (a) Anseth, K. S.; Bowman, C. N. *Polym. React. Eng.* **1993**, *1*, 499. (b) Anseth, K. S.; Wang, C. M.; Bowman, C. N. *Macromolecules* **1994**, *27*, 650. (c) Young, J. S.; Bowman, C. N. *Macromolecules* **1999**, *32*, 6073.

(4) Wen, M.; McCormick, A. V. *Macromolecules* **2000**, *33*, 9247.

(5) Goodner, M. D.; Bowman, C. N. *Macromolecules* **1999**, *32*, 6552.

(6) Berchtholt, K. A.; Hacioglu, B.; Lovell, L. G.; Nie, J.; Bowman, C. N. *Macromolecules* **2001**, *34*, 5103.

(7) (a) Hutchinson, J. B.; Anseth, K. S. *Polym. Prepr.* **2000**, *41*, 1326. (b) Lu, H.; Lovell, L. G.; Bowman, C. N. *Macromolecules* **2001**, *34*, 8021.

(8) (b) Elliot, J. E.; Bowman, C. N. *Macromolecules* **1999**, *32*, 8621. (b) Elliot, B. J.; Willis, W. B.; Bowman, C. N. *Macromolecules* **1999**, *32*, 3201. (c) Elliot, B. J.; Scranton, A. B.; Cameron, J. H.; Bowman, C. N. *Chem. Mater.* **2000**, *12*, 633.

(9) (a) Elliot, J. E.; Bowman, C. N. *Macromolecules* **2001**, *34*, 4642. (b) Lovell, L. G.; Stansburry, J. W.; Syrpes, D. C.; Bowman, C. N. *Macromolecules* **1999**, *32*, 3913.

(10) Dong, S.; Wei, Y.; Zhang, Z. K. *J. Appl. Polym. Sci.* **1999**, *74*, 516.

(11) (a) Decker, C.; Decker, D. *Polymer* **1997**, *38*, 2229. (b) Decker, C.; Morel, F.; Decker, D. *Proceedings PRA Radcure Coatings and Inks: Curing and Performance*, 1998; paper 3. (c) Decker, C.; Bianchi, C.; Morel, F.; Jonsson, S.; Hoyle, C. *Conference Proceedings Radtech Europe*, 1999; p 447. (d) For a review concerning photoinitiated polymerizations see: Decker, C. *Mater. Sci. Technol.* **1997**, *18*, 615. For the determination of kinetic constants see: (e) Decker, C.; Moussa, K. *Polym. Prepr.* **1988**, *29*, 516. (f) Decker, C.; Moussa, K. *Eur. Polym. J.* **1990**, *26*, 393. (g) Decker, C.; Moussa, K. *Makromol. Chem.* **1990**, *191*, 963. (h) Decker, C. *Macromolecules* **1990**, *23*, 5217. (i) Decker, C.; Moussa, K. *J. Coat. Technol.* **1990**, *62*, 55. (j) Decker, C. *J. Polym. Sci., Part A: Polym. Chem.* **1992**, *30*, 913. (k) Decker, C. *Spec. Publ.—R. Soc. Chem.* **1993**, *125*, 32.

(12) Brill, R. P.; Palmese, G. R. *J. Appl. Polym. Sci.* **2000**, *76*, 1572.

(13) Decker, C.; Moussa, K. *Makromol. Chem.* **1988**, *189*, 2381.

(14) (a) Chalmers, J.; Dent, G. *Industrial Analysis with Vibrational Spectroscopy*; Royal Society of Chemistry: London, 1997; p 228. (b) Griffiths, P. In *Laboratory Methods in Vibrational Spectroscopy*, 3rd ed.; Willis, H., van der Maas, J., Miller, R., Eds.; J. Wiley: Chichester, UK, 1987; Chapter 6. (c) Gold, H.; Rechsteiner, C.; Buck, P. *Anal. Chem.* **1976**, *48*, 1540.

(15) (a) Windig, W.; Guilment, J. *Anal. Chem.* **1991**, *63*, 1452. (b) Guilment, J.; Markel, S.; Windig, W. *Appl. Spectrosc.* **1994**, *48*, 320. (c) Windig, W. *Chemometrics and Intelligent Laboratory Systems* **1994**, *23*, 71. (d) SIMPLISMA: SIMPLISMAx software package developed by Windig, W.; Eastman Chemical Co., Rochester, NY 14652-3712.

(16) (a) Tauler, R.; Barcelo, D. *TRAC Trends Anal. Chem.* **1993**, *12*, 319. (b) Tauler, R.; Kowalski, B. *Anal. Chem.* **1993**, *65*, 2040. (c) Tauler, R.; Smilde, A. K.; Henshaw, J. M.; Burgess, L. W.; Kowalski, B. R. *Anal. Chem.* **1994**, *66*, 3337.

(17) (a) Schoonover, R.; Marx, R.; Zhang, S. L. *Appl. Spectrosc.* **2003**, *57*, 155A. (b) Tauler, R.; Smilde, A. K.; Henshaw, J. M.; Burgess, L. W.; Kowalski, B. R. *Anal. Chem.* **1994**, *66*, 3337. (c) MCR: a tool in PLS_toolbox 3.0.; Eigenvector Research Inc., Manson, WA 98831.

(18) For a detailed theoretical description see: (a) Noda, I. *Appl. Spectrosc.* **2000**, *54*, 994. (b) Noda, I. *Appl. Spectrosc.* **1993**, *47*, 1329. For a description of some applications see: (c) Murayama, K.; Czarnik-Matusewicz, B.; Wu, Y.; Tsenkova, R.; Ozaki, Y. Appl. *Spectrosc.* **2000**, *54*, 978. (d) Ren, Y.; Murakami, T.; Nishioka, T.; Nakashima, K.; Noda, I.; Ozaki, Y. *J. Phys. Chem. B* **2000**, *104*, 679. Ozaki, Y.; Wang, Y. *J. Near Infrared Spectrosc.* **1998**, *6*, 19. (e) Buchet, R.; Wu, Y.; Raimbault, C.; Ozaki, Y. *Appl. Spectrosc.* **2001**, *55*, 155. (f) Šaiš, S.; Amari, T.; Ozaki, Y. *Anal. Chem.* **2001**, *73*, 5184. For a critical evaluation of the use of 2D correlation spectroscopy see: (g) Huang, H.; Malkov, S.; Coleman, M.; Painter, P. *Macromolecules* **2003**, *36*, 8148. (h) Huang, H.; Malkov, S.; Coleman, M.; Painter, P. *Macromolecules* **2003**, *36*, 8156.

(19) For a detailed description about the RT-FTIR equipment used see: Dias, A. A.; Hartwig, H.; Jansen, J. F. G. A. *Surf. Coat. Int., JOCCA* **2000**, *83*, 382.

(20) (a) Kelen, T.; Tudos, F. *J. Macromol. Sci., Chem.* **1975**, *A9*, 1 For a nice example see: Liang, D. J.; Sang, H.-H. *J. Polym. Sci., Part A: Polym. Chem.* **1999**, *37*, 1789. (b) van Herk, A. M.; Droge, T. *Macromol. Theory Simul.* **1997**, *6*, 1263.

(21) (a) Davis, T. P. *J. Polym. Sci., Part A: Polym. Chem.* **2001**, *39*, 697. (b) Landry, R.; Pendlis, A.; Deuver, T. A. *J. Polym. Sci., Part A: Polym. Chem.* **2000**, *38*, 2319. (c) Jenkins, A. D. *Macromol. Rapid Commun.* **1996**, *17*, 275. (d) Gao, J. Pendlis, A. *J. Macromol. Sci., Rev. Macromol. Chem. Phys.* **1998**, *C38*, 651.

(22) Homopolymerization of some fumarates is known. See: Cohin, D.; Laschewesky, A.; Pantousiert, N. *Polymer* **2000**, *41*, 3895.

(23) The fumarate−maleate isomerization has not been described previously although the thermal isomerization of maleate into fumarate during the synthesis of unsaturated polyesters is well-known.Furthermore, it is known that maleates can isomerize with radicals in high yields to fumarates for instance under the influence thiyl radicals generated from phenyl dithiane during irradiation. See: Harrowven, D. C.; Hannam, J. C. *Tetrahedron* **1999** *55*, 9341.

(24) (a) Xi, H.; Basset, W., Jr.; Vogl, O. *J. Polym. Sci., Polym. Chem.* **1983**, *21*, 891. (b) Mantranga, C.; Meij, E. *Angew. Macromol. Chem.* **1998**, *256*, 1.

(25) (a) Teddder, J. M. *Angew. Chem., Int. Ed. Engl.* **1982**, *21*, 401. (b) Tedder, J. M.; Walton, J. C. *Tetrahedron* **1980**, *36*, 701.

(26) Such a charge-transfer complex between an unsaturated polyester and triethylene glycol divinyl ether has been observed using fluorescence spectroscopy. See: Zhang, L.; Liu, L.; Chen, Y. *J. Appl. Polym. Sci.* **1999**, *74*, 3541.

(27) Greenley, R. Z. In *Polymer Handbook*, 4th ed.; Brandrup, J., Immergut, E. H., Grulke, E. A., Eds.; Wiley-Interscience: New York, 1999; Chapter II, p 181.

(28) Jung, S.-J.; Lee, S.-J.; Cho, W.-J.; Ha, C.-S. *J. Appl. Polym. Sci.* **1998**, *69*, 695. (b) Shi, W.; Ranby, B. *J. Appl. Polym. Sci.* **1994**, *51*, 1129.

(29) Pohl, H. U.; Treanckner, H.-J.; Rosenkranz, H. J. *Angew. Macromol. Chem.* **1981**, *98*, 1.

(30) (a) Smith, T. J.; Shemper, B. S.; Nobles, J. S.; Casanova, A. M.; Ott, C.; Mathias, L. J. *Polymer* **2003**, *44*, 6211. (b) Smith, T. J.; Shemper, B. S.; Nobles, J. S.; Casanova, A. M.; Ott, C.; Mathias, L. J. *Polym. Prepr.* **2003**, *44*, 119. (c) Smith, T. J.; Mathias, L. J. *Biomacromolecules* **2002**, *3*, 1392. (d) Mathias, L. J.; Thigpen, K.; Avci, D. *Macromolecules* **1995**, *28*, 8872. (e) Mathias, L. J.; Kusefoglu, S. H.; Kress, A. O. *Macromolecules* **1987**, *20*, 2326. (f) Mathias, L. J.; Kusefoglu, S. H. *J. Polym. Sci., Part C: Polym. Lett.* **1987**, *25*, 451. EHMA is now commercial available from Nippon Shokubai Co. (Tokyo).

(31) Krause, T.; Schmidt-Naake, G. *Angew. Macromol. Chem.* **1998**, *258*, 83. See also ref 26.

(32) For 2-bromoethyl methacrylate−vinyl butyl ether $r_1 = 14$, $r_2 = 0$ were found; however, for methyl methacrylate−vinyl ethyl ether $r_1 = 37$, $r_2 = 0$ were found (ref 26).

(33) (a) Pulsed laser polymerization data (PLP): methyl methacrylate−butyl acrylate $r_1 = 2.6$, $r_2 = 0.4$; dodecyl methacrylate−methyl acrylate $r_1 = 2.4$, $r_2 = 0.2$. Methyl methacrylate−dodecyl acrylate $r_1 = 3.3$, $r_2 = 0.4$. BuBack, M.; Felderman, A.; Barner-Kowollik, C.; Lacik, I. *Macromolecules* **2001**, *34*, 5439. (b) PLP data: methyl methacrylate−butyl acrylate $r_1 = 2.1$, $r_2 = 0.4$. Hutchinson, R. A.; McMinn, J.; Paquet, D. A., Jr.; Beuermann, S.; Jackson, C. *Ind. Eng. Chem. Res.* **1997**, *36*, 1103. (c) ^{1}H NMR: HEMA−*tert*-butyl acrylate $r_1 = 1.8$, $r_2 = 0.5$. Martinez, G.; Sanchez-Chaves, M.; Madruga, E. L.; Fernandez-Monreal, C. *Polymer* **2000**, *41*, 6021. (d) Methyl methacrylate−methyl acrylate $r_1 = 2.0$, $r_2 = 0.4$. Jager, W. F.; Lungu, A.; Chen, D. Y.; Neckers, D. C. *Macromolecules* **1997**, *30*, 780. See also ref 26.

(34) Odian, G. *Principles of Polymerization*, 3rd ed.; J. Wiley & Sons: New York, 1991.

(35) (a) $r_1 = 5.9$, $r_2 = 0.01$; ref 26. (b) For the copolymerization of a methacrylated salicyl derivative with NVP see: Buaduin, G.; Boutevin, B.; Belbachir, M.; Meghabar, R. *Macromolecules* **1995**, *28*, 1750.

(36) (a) Miller, C. W.; Jonsson, S.; Hoyle, C. E.; Yang, D.; Kuang, W. F.; Iijima, T.; Nason, C.; Ng, L.-T. *Proc. Radtech North America* **2000**, 754. (b) Miller, C. W.; Kess, R.; Iijima, T.; Hoyle, C. E. *Polym. Prepr.* **1997**, *38*, 258. (c) Miller, C. W.; Hoyle, C. E.; Jonsson, S.; Nason, C.; Lee, T. Y.; Kuang, W. F.; Viswanathan, K. *ACS Symp. Ser.* **2003**, *847*, 2.

(37) (a) Jansen, J. F. G. A.; Dias, A. A.; Dorschu, M.; Coussens, B. *Polym. Prepr.* **2001**, *42*, 769. (b) Jansen, J. F. G. A.; Dias, A. A.; Dorschu, M.; Coussens, B. *Macromolecules* **2002**, *35*, 7529. (c) Jansen, J. F. G. A.; Dias, A. A.; Dorschu, M.; Coussens, B. Patent WO 02/42383. (d) Jansen, J. F. G. A.; Dias, A. A.; Dorschu, M.; Coussens, B. *Macromolecules* **2003**, *36*, 3861. (e) Jansen, J. F. G. A.; Dias, A. A.; Dorschu, M.; Coussens, B. *ACS Symp. Ser.* **2003**, *847*, 127.

MA035587R